AMERICAN SOCIETY FOR MICROBIOLOGY | mSystems®

RESEARCH ARTICLE
Host-Microbe Biology

Global Assessment of *Mycobacterium avium* subsp. *hominissuis* Genetic Requirement for Growth and Virulence

Marte S. Dragset,[a,b,c,d] Thomas R. Ioerger,[e] Maja Loevenich,[a,b] Markus Haug,[a,b,f] Niruja Sivakumar,[a,b] Anne Marstad,[a,b] Pere Joan Cardona,[c] Geir Klinkenberg,[g] Eric J. Rubin,[d] Magnus Steigedal,[a,b,d,f] Trude H. Flo[a,b]

[a]Centre of Molecular Inflammation Research, Norwegian University of Science and Technology, Trondheim, Norway
[b]Department of Clinical and Molecular Medicine, Norwegian University of Science and Technology, Trondheim, Norway
[c]Tuberculosis Research Unit, Germans Trias i Pujol Research Institute, Badalona, Barcelona, Spain
[d]Department of Immunology and Infectious Diseases, Harvard T. H. Chan School of Public Health, Boston, Massachusetts, USA
[e]Department of Computer Science and Engineering, Texas A&M University, College Station, Texas, USA
[f]Department of Infection, St. Olavs University Hospital, Trondheim, Norway
[g]Department of Biotechnology and Nanomedicine, SINTEF Materials and Chemistry, Trondheim, Norway

ABSTRACT Nontuberculous mycobacterial infections caused by the opportunistic pathogen *Mycobacterium avium* subsp. *hominissuis* (MAH) are currently receiving renewed attention due to increased incidence combined with difficult treatment. Insights into the disease-causing mechanisms of this species have been hampered by difficulties in genetic manipulation of the bacteria. Here, we identified and sequenced a highly transformable, virulent MAH clinical isolate susceptible to high-density transposon mutagenesis, facilitating global gene disruption and subsequent investigation of MAH gene function. By transposon insertion sequencing (TnSeq) of this strain, we defined the MAH genome-wide genetic requirement for virulence and *in vitro* growth and organized ~3,500 identified transposon mutants for hypothesis-driven research. The majority (96%) of the genes we identified as essential for MAH *in vitro* had a mutual ortholog in the related and highly virulent *Mycobacterium tuberculosis* (*Mtb*). However, passaging our library through a mouse model of infection revealed a substantial number (54% of total hits) of novel virulence genes. More than 97% of the MAH virulence genes had a mutual ortholog in *Mtb*. Finally, we validated novel genes required for successful MAH infection: one encoding a probable major facilitator superfamily (MFS) transporter and another encoding a hypothetical protein located in the immediate vicinity of six other identified virulence genes. In summary, we provide new, fundamental insights into the underlying genetic requirement of MAH for growth and host infection.

IMPORTANCE Pulmonary disease caused by nontuberculous mycobacteria is increasing worldwide. The majority of these infections are caused by the *Mycobacterium avium* complex (MAC), whereof >90% are due to *Mycobacterium avium* subsp. *hominissuis* (MAH). Treatment of MAH infections is currently difficult, with a combination of antibiotics given for at least 12 months. To control MAH by improved therapy, prevention, and diagnostics, we need to understand the underlying mechanisms of infection. Here, we provide crucial insights into MAH's global genetic requirements for growth and infection. We find that the vast majority of genes required for MAH growth and virulence (96% and 97%, respectively) have mutual orthologs in the tuberculosis-causing pathogen *M. tuberculosis* (*Mtb*). However, we also find growth and virulence genes specific to MAC species. Finally, we validate novel mycobacterial virulence factors that might serve as future drug targets for MAH-specific treatment or translate to broader treatment of related mycobacterial diseases.

Citation Dragset MS, Ioerger TR, Loevenich M, Haug M, Sivakumar N, Marstad A, Cardona PJ, Klinkenberg G, Rubin EJ, Steigedal M, Flo TH. 2019. Global assessment of *Mycobacterium avium* subsp. *hominissuis* genetic requirement for growth and virulence. mSystems 4:e00402-19. https://doi.org/10.1128/mSystems.00402-19.

Editor Ileana M. Cristea, Princeton University

Address correspondence to Marte S. Dragset, marte.dragset@ntnu.no.

Marte S. Dragset and Thomas R. Ioerger contributed equally to this work. Author order was determined alphabetically.

Received 2 July 2019
Accepted 14 November 2019
Published 10 December 2019

KEYWORDS conditionally required genes, *Mycobacterium avium*, *Mycobacterium tuberculosis*, transposon insertion sequencing, virulence genes

Mycobacterium avium complex (MAC) is a group of genetically related and ubiquitously distributed opportunistic mycobacteria that can cause nontuberculous infections collectively called MAC disease (1). *M. avium* (*Mav*), one of the MAC species, has been classified into subspecies *avium*, *paratuberculosis*, *silvaticum*, and *hominissuis* based on molecular characterizations, prevalent hosts, and diseases caused (2, 3). The latter subspecies, *M. avium* subsp. *hominissuis* (MAH), can infect humans and lead to pulmonary and disseminated disease, particularly, but not only, in immunocompromised individuals (4). MAH infections are currently hard to treat, with a combination of antibiotics typically given for at least 12 months (5). Similar to its relative *M. tuberculosis* (*Mtb*), the causative agent of tuberculosis, MAH proliferates within macrophages by hijacking normal phagosomal trafficking, overcoming the host's elimination strategies (6–12). Mechanisms of infection may therefore partly be conserved between the two species. MAH lacks the type VII ESX-1 secretion system crucial for full *Mtb* virulence (13), suggesting that they also differ in virulence strategies. While *Mtb* is an obligate human pathogen in nature, with limited survival outside the host, *Mav* is environmental and opportunistic, found in a variety of niches (e.g., soil, freshwater, showerheads) and a range of prevalent hosts (3). MAH isolates exhibit high genetic variation (14), perhaps as an adaptation to diverse niches and hosts. It is currently not known to what degree MAH and *Mtb* depend on similar mechanisms for growth and virulence, given the same selective conditions. Even so, MAH genes encoding factors required for basic proliferation and virulence may be attractive targets for improved MAH therapies and may translate to the treatment of related mycobacterial diseases.

Transposon insertion sequencing (TnSeq), which combines transposon mutagenesis and massive parallel sequencing, has been widely used to determine the conditional requirement of bacterial genes on a genome-wide scale (15). By massive parallel sequencing of libraries consisting of more than 100,000 transposon mutants, the genetic requirements of *Mtb*, *M. marinum*, and *M. avium* subsp. *paratuberculosis* have been defined for *in vitro* growth or infection (16–20). For research on MAH gene function, transposon mutagenesis has also been of great importance (21–29), although the libraries screened have been limited in size ($<$5,000 mutants). The first MAH strain with a publicly available, fully assembled genome, was MAH 104 (30). This strain has thus, naturally, been widely studied (e.g., references 8, 10, 11, 30, and 31). MAH 104 is, along with many other *Mav* strains, resistant to transduction by mycobacteriophage TM4 (32), the progenitor of ϕMycoMarT7 (the phage used to generate high-density transposon libraries in other mycobacterial species [16–20, 33, 34]), and transforms with low efficiency (28, 35–37). Therefore, to facilitate genetic engineering and genome-wide investigation of MAH gene function, we identified an MAH strain (MAH 11) highly susceptible to both ϕMycoMarT7-mediated transposon mutagenesis and transformation (another strain, MAH A5, was recently shown to be transducable by ϕMycoMarT7 as well [26, 27]). We used MAH 11 to generate a high-density transposon insertion library (170,000 mutants) with ~66% saturation density, which we profiled for genes required *in vitro* and in a mouse model of infection. In fact, MAH 11 is currently used as a screening strain in mycobacterial drug discovery programs (38, 39), adding further value to determining the growth requirements of this particular strain. Moreover, we constructed an ordered subset of our transposon library, providing access to ~3,500 MAH mutants, with which we validated novel MAH virulence factors (the overall experimental setup of our study is summarized in Fig. 1).

RESULTS

MAH 11 is susceptible to high-density transposon mutagenesis and transformation. We aimed to find an MAH strain in which we could create high-density transposon mutant libraries. The transposon donor phagemid ϕMycoMarT7 is widely used (and recommended over Tn*5367* transposition [33]) for efficient mycobacterial

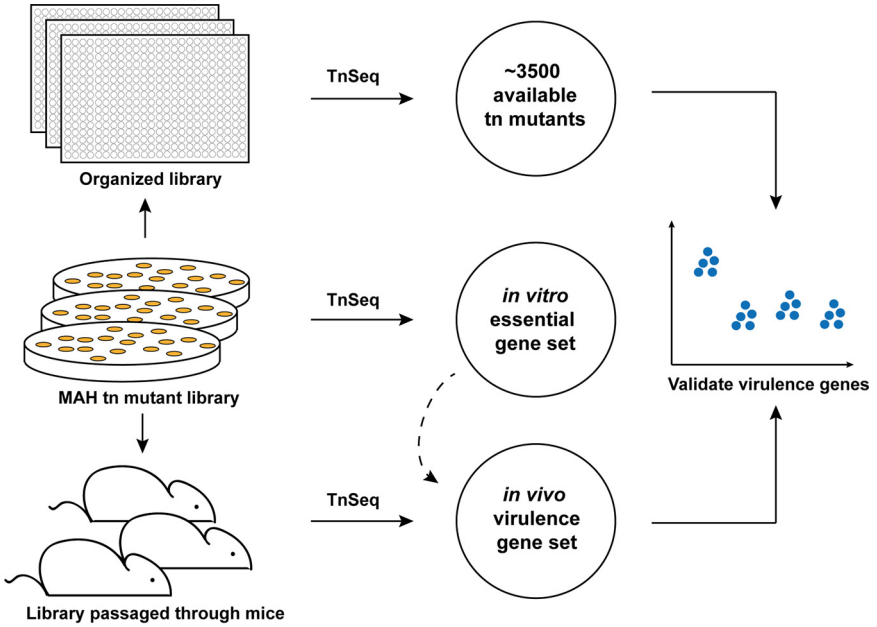

FIG 1 Experimental setup of the study. An *M. avium* subsp. *hominissuis* (MAH) transposon mutant library of 170,000 mutants (~66% coverage) was generated by selection on 7H10 agar medium. This library was further subjected to mouse infection or organized mutant by mutant on 384-well plates (24 plates). By TnSeq of the *in vitro*-selected (7H10), *in vivo*-selected (C57BL/6 mice), and the organized library, the MAH essential gene set, and virulence gene sets were defined, and the locations of ~3,500 organized mutations were identified. The output from the *in vitro*-selected TnSeq library was used to identify virulence genes (dashed line). Finally, a subset of virulence gene hits was validated by mouse infection experiments. Tn, transposon.

transposon mutagenesis (16–20, 34). ϕMycoMarT7 is derived from ϕAE87, which originates from mycobacteriophage TM4 (34, 40). TM4 has been inconsistent in its ability to transduce various *Mav* strains and is unable to infect the commonly studied genome-sequenced strain MAH 104 (32). In agreement with these observations, we failed to obtain kanamycin-resistant mutants (marker for successful transposition of the ϕMycoMarT7-encoded *Himar1* transposon) when attempting to transduce MAH 104. Hence, to identify a ϕMycoMarT7-transducible strain of MAH, we screened seven in-house clinical *Mav* isolates originating from patients at the National Taiwan University Hospital, Taiwan. Around 70% of the strains resulted in various numbers of kanamycin-resistant colonies after transduction, indicating *Himar1* transposition. On the basis of its particularly efficient transducibility (up to 300,000 kanamycin-resistant colonies per ml starting culture in our initial small-scale screen) and general ease to handle, we focused on a strain isolated from an HIV-positive patient's bone marrow, MAH 11.

Mav is notoriously hard to transform (28, 35–37), complicating introduction of new DNA and thus genetic engineering of this species. In our and others' experience, strain MAH 104 is transformable with low efficiency (36, 41). We investigated the transformation frequency of MAH 11 and found that this strain is around 100 times more susceptible to obtain plasmid DNA compared to the MAH 104 strain, using optimized protocols for *Mav* electroporation (Fig. 2A) (35). In summary, MAH 11 might be particularly apt for high-density transposon mutagenesis and hypothesis-driven genetic approaches.

MAH 11 genome sequence. We sequenced the genome of the ϕMycoMarT7-transducible MAH 11 strain on an Illumina HiSeq 2500 instrument in paired-end mode with a read length of 125 bp, yielding a mean depth of coverage of 55.4. The sequence was assembled by a comparative assembly strategy, using MAH 104 as a reference sequence, augmented with contig building to build large-scale indels. The Illumina data were supplemented with long reads (up to 40 kb) from a PacBio sequencer, which were

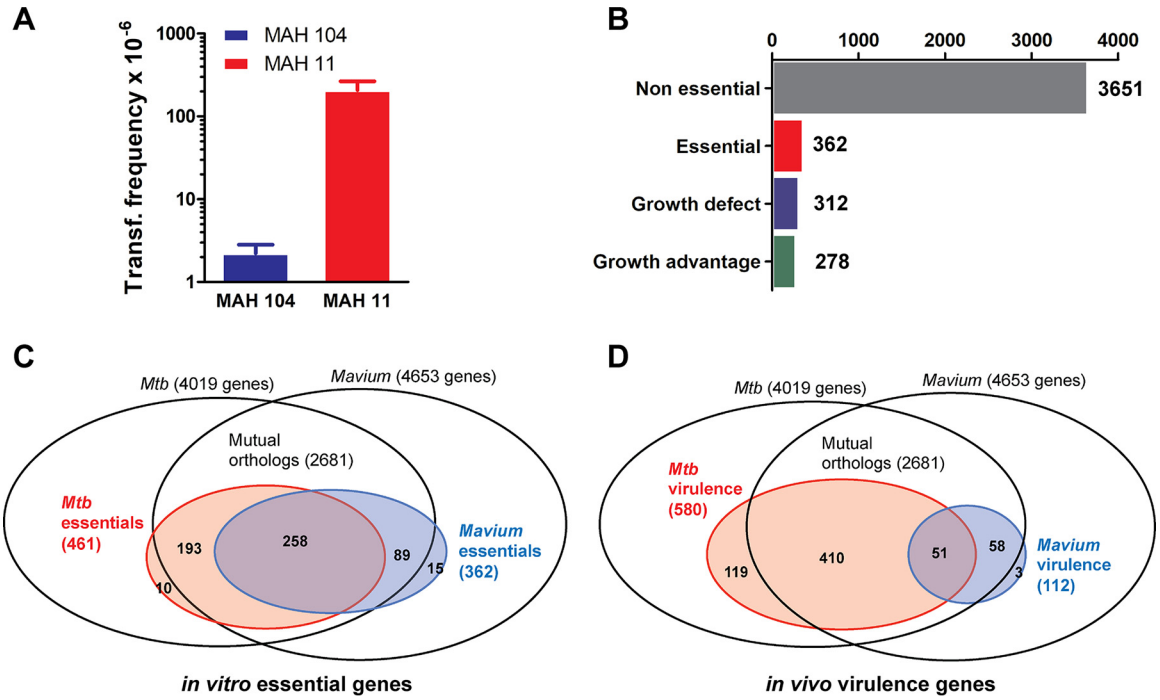

FIG 2 MAH *in vitro* essential and *in vivo* virulence gene sets. (A) MAH 11 and MAH 104 transformation frequencies. Data show means plus standard errors of the means (SEM) (error bars) for three individually electroporated samples. The results are representative of two independent experiments. (B) Number of MAH 11 genes defined as essential, growth defect, growth advantage, and nonessential. (C) Venn diagram illustrating MAH 11 and *Mtb* (as defined by DeJesus et al. [53]) *in vitro* essential genes, relative to the entire pool of MAH 11 (4,653) and *Mtb* (4,019) genes and their mutual orthologs (2,681). MAH 11 (362) and *Mtb* (461) essential genes are shown within the blue and red circles, respectively. A total of 258 genes are essential in both species, 89 (MAH 11) and 193 (*Mtb*) essential genes have a nonrequired mutual ortholog in the other species, and 15 (MAH 11) and 10 (*Mtb*) essential genes do not have mutual orthologs in the other species. (D) Venn diagram illustrating MAH 11 and *Mtb in vivo* virulence (as defined by Zhang et al. [16]) in C57BL/6 mice. MAH 11 (112) and *Mtb* (580) virulence genes are shown within the blue and red circles, respectively. Fifty-one genes cause virulence in both species, 58 (MAH 11) and 410 (*Mtb*) virulence genes have a mutual ortholog in the other species not required for virulence in TnSeq screening, and 3 (MAH 11) and 119 (*Mtb*) virulence genes do not have mutual orthologs in the other species.

used to confirm the connectivity of the chromosome. The length of the genome is 5,098,805 bp, and the genome is GC-rich (69.2%) like that of other mycobacteria (Fig. 3A). The genome sequence is highly concordant with the recently reported draft genome of MAH 11 (70 contigs) (42).

MAH 11 is positively identified as *M. avium* subsp. *hominissuis*, based on 16S rRNA and *hsp65* sequences that are identical to those of MAH 104 (but distinct from other subspecies, like *M. avium* subsp. *avium*) (2). However, relative to MAH 104, there are substantial numbers of single nucleotide polymorphisms (SNPs) (approximately 10 SNPs per 1 kb) and a cumulative loss of ~377 kb, showing that it is a distinct lineage (Fig. 3E). The reductions are clustered in several large-scale deletions, listed in Table 1. This variability has been seen in other *Mav* isolates (43, 44), and several of the large-scale deletions correspond to known large-scale polymorphisms (43). In addition, there are several large-scale insertions (Table 1), including a prophage (56 genes, *b6k05_17725-18015*, inserted at coordinate 3.77 Mbp), and a cluster of 48 nonphage metabolic genes (*b6k05_03885-04170*; 57 kb). The MAH 11 genome contains at least 14 copies of IS*1245* (similar to MAH 104 [45]), but none of IS*901* (associated with members of the MAC complex primarily infecting birds [43, 46]). Figure 3B shows the position of MAH 11 in a phylogenetic tree (created using PHYLIP [http://evolution.genetics.washington.edu/phylip.html]) together with 21 other *M. avium* genomes obtained from NCBI GenBank, including *M. avium* subsp. *paratuberculosis* (MAP) K10 and three *M. avium* subsp. *avium* (MAA) as outgroup strains.

We identified 4,653 open reading frames (ORFs) (along with 1 copy of the rRNAs [16S, 23S, 5S] and 42 tRNAs, similar to MAH 104) using the NCBI Prokaryotic Genome

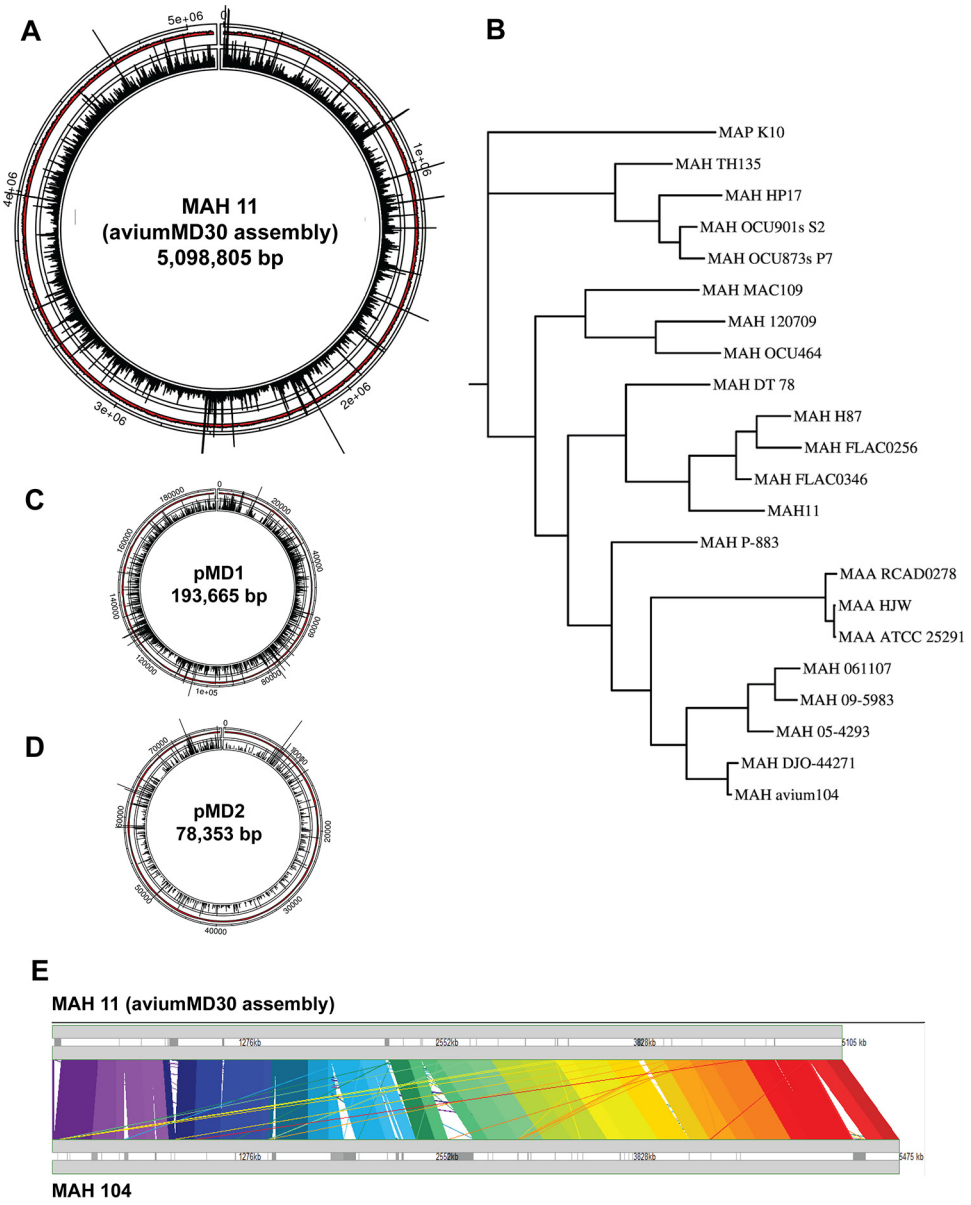

FIG 3 MAH 11 genome and distribution of transposon insertion counts. (A) Transposon insertion counts across the MAH 11 genome. The height of the black bars represents the number of insertion counts at the respective genome site. (B) MAH 11 in a phylogenetic context with 21 other *M. avium* genomes obtained from NCBI GenBank. (C and D) Transposon insertion counts in pMD1 (C) and pMD2 (D). (E) Comparison of MAH 11 and MAV 104 genomes. Synteny plot showing local sequence homologies between MAH 11 and MAV 104 across the entire lengths of each genome (5.1 Mb and 5.5 Mb, respectively), made with M-GCAT software (77). This plot illustrates that most genes in MAH 11 are present in MAH 104, and the gene order has largely been preserved (i.e., no large-scale chromosomal rearrangements). However, several large regions were deleted (along a few large-scale insertions), and thus, MAH 11 has undergone a substantial reduction of 377 kb in net size.

Annotation Pipeline (47). A total of 4,209 genes have mutual orthologs with MAH 104 (where each gene in one organism is the best match for the ortholog in the other organism, with a BLAST E value of $<10^{-10}$; see Data Set S1A in the supplemental material). Almost all of these orthologs (4,123) have ≥96% amino acid identity, and nearly half (1,730) have 100% amino acid identity. For simplicity, we will, where applicable, refer to MAH ORFs using the MAH 104 locus tags (*mav_xxxx*) from here on. Compared to *Mtb* (H37Rv), MAH 11 has ~500 more genes, and more than half the genes in each genome (2,681) have a mutual ortholog in the other genome (67% of *Mtb* and 58% of MAH total genes) (Fig. 2C and Data Set S1C). Most of the remaining genes

TABLE 1 All insertions and deletions of >10 kb in MAH 11 relative to MAH 104[a]

Insertion or deletion >10 kb	Coordinate (MAH 11)	Size (bp)	Annotation
Insertions > 10 kb			
B6K05_11270−B6K05_11320	2378550	10,989	Metabolic genes
B6K05_05585−B6K05_05635	1099353	11,986	Metabolic genes
B6K05_10305−B6K05_10440	2149613	29,719	Hypothetical, transporters
BK065_17725−BK065_18015	3779806	41,431	New prophage
BK065_00050−BK065_00255	11154	45,910	Hypothetical, transposases
BK065_03885−BK065_04170	756785	57,435	Metabolic genes
Deletions > 10 kb			
MAV_0683−MAV_0700	639611	10,375	LSP12
MAV_2247−MAV_2267	2068693	14,126	
MAV_2217−MAV_2235	2052758	21,283	LSP10
MAV_1450−MAV_1479	1445064	23,908	LSP14
MAV_0471−MAV_0508	463246	31,473	LSP7
MAV_0253−MAV_0299	293034	40,100	LSP3
MAV_5026−MAV_5107	4888896	81,635	LSP6
MAV_1806−MAV_1974	1800387	162,713	LSP4
MAV_2518−MAV_2691	2378550	173,202	LSP1

[a]Eight of the >10-kb deletions can be identified with a previous defined list of 14 known LSPs (large-scale polymorphisms) among *M. avium* strains (43). The remaining six LSPs were present in the MAH 11 genome.

also have orthologs, but their E values are above the stringent threshold of 10^{-10} (i.e., 1,052 MAH genes have no clear *Mtb* ortholog [Data Set S1C]), or their specific partner in the other genome is ambiguous, as is sometimes the case in duplicated gene families.

MAH 11 plasmids. Two large extrachromosomal contigs that appear to represent circular plasmids were detected. One, pMD1 (193 kb, 162 ORFs) (Fig. 3C and Data Set S1D), bears weak similarity (based on BLAST search) to parts of plasmids in a wide range of other mycobacteria. The other, pMD2 (78 kb, 66 ORFs) (Fig. 3D and Data Set S1E), is nearly identical to conjugative plasmid pMA100 from MAH strain 88Br (though reduced, since pMA100 is 116 kb [Data Set S1F]) (48) and bears partial similarity to the conjugative pRAW-like plasmids found in several slow-growing mycobacterial species (49).

MAH *in vitro* essential gene set. To define genes required for MAH *in vitro* growth, we generated, by ϕMycoMarT7-mediated transduction, a library of ~170,000 transposon mutants selected on 7H10 medium. The *Himar1*-based mariner transposon of ϕMycoMarT7 inserts randomly at TA dinucleotides (50), of which there are 55,516 sites in the MAH 11 genome (excluding plasmids). We sequenced the transposon junctions of two independent DNA libraries, mapped the genomic positions of the transposon insertion sites (insertion counts), and counted insertions (reduced to unique templates using barcodes [51]) (see Table S1 in the supplemental material). The library had a saturation of 66.3%, with insertions at 36,813 out of 55,516 TA sites. By gene requirement analysis, using a hidden Markov model incorporated into the TRANSIT platform (52), we defined 362 genes as essential for *in vitro* growth, 312 as genes causing growth defects when disrupted, 278 as genes causing growth advantage when disrupted, and 3651 genes as nonessential for growth (Fig. 2B and Data Set S1G). Seventy-one percent (258/362) of MAH 11's essential genes had an essential ortholog in *Mtb* (as defined by DeJesus et al. [53]). Remarkably, very few MAH (15) and *Mtb* (10) essential genes (~4% and ~2% of total essential genes, respectively) did not have a mutual ortholog in the other species (Fig. 2C and Data Set S1G), suggesting that the vast majority of genes required for *in vitro* proliferation are conserved in MAH and *Mtb*.

Almost all genes found on the two MAH 11 plasmids were nonessential for *in vitro* growth (Data Sets S1H and S1I). However, on pMD1, four genes were defined as causing growth defects (though a decrease in insertion counts probably reflects a loss of the plasmid rather than a reduction in growth rate) when disrupted: two genes encoding hypothetical proteins, one homologous to a gene encoding chromosome partitioning protein, *parB*, and one homologous to the DNA processing protein-encoding *dprA*. On

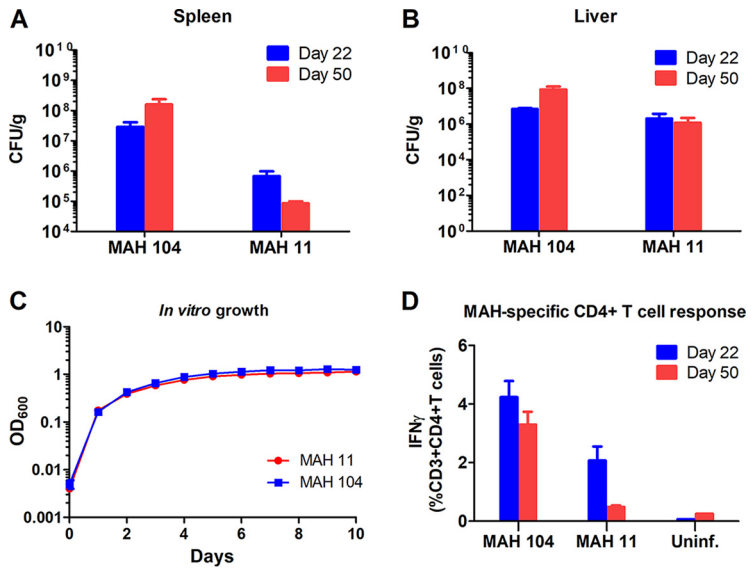

FIG 4 MAH 11 and MAH 104 mouse model infection. (A and B) Bacterial burden in spleen (A) and liver (B) of mice after 22 and 50 days of infection with MAH 104 and MAH 11. Data show means plus SEM for four infected mice in each group. (C) MAH 104 and MAH 11 *in vitro* growth (7H9 medium). Data show means ± SEM for three replicate samples per condition. The results are representative of two independent experiments. (D) Frequencies of MAH-specific $CD4^+$ T cells after 22 and 50 days of MAH 104 and MAH 11 infection. Splenocytes from all mice were stimulated overnight with MAH, and frequencies of IFN-γ-producing $CD4^+$ effector T cells were analyzed by flow cytometry. Data show means plus SEM for four infected mice per group. Mouse experiments are representative of two independent experiments (for 50 day time point). Uninf., uninfected.

pMD2, a gene homologous to *rep*, involved in plasmid replication, caused growth defect when disrupted. Taken together, 674 chromosomal and 5 plasmid MAH genes were defined as essential or causing a growth defect *in vitro* when disrupted.

MAH 11 establishes infection in mice. We and others have shown that MAH 104 is virulent in mice (8, 11, 12, 22). We thus examined whether MAH 11 would be suitable to study the role of MAH genes *in vivo*. C57BL/6 mice were infected intraperitoneally with MAH 11 or MAH 104, and organ bacterial load was analyzed in the chronic phase of infection. As we have previously shown, bacterial loads remained relatively constant in liver and spleen from 22 to 50 days after initial MAH 104 infection (12). The same trend was seen for MAH 11, albeit with an overall lower bacterial load compared to that of MAH 104, especially in the spleen (Fig. 4A and B). MAH 11 and MAH 104 grew comparably in 7H9 medium (Fig. 4C), suggesting that MAH 11 is less virulent than MAH 104 in C57BL/6 mice.

T cells produce effector cytokines upon activation to elicit an adaptive immune response toward infections. To control *Mav* infection, production of gamma interferon (IFN-γ) effector cytokine by $CD4^+$ T helper 1 cells is of particular importance (54). We have previously monitored antimycobacterial T cell responses to MAH 104 (12). To investigate whether MAH 11 is suitable for studying MAH-specific host immune responses, we measured mycobacterium-specific $CD4^+$ T cell responses after mouse infection. Figure 4D shows the frequencies of MAH-specific $CD4^+$ T helper 1 cells producing IFN-γ effector cytokine after infection. Interestingly, the frequencies of IFN-γ-producing $CD4^+$ T cells were found to be lower in MAH 11-infected mice than in MAH 104-infected mice after 50 days of infection, possibly reflecting the lower organ bacterial loads (Fig. 4A and B).

We performed a broader characterization of the inflammation and tissue pathology in MAH 11-infected mice at day 26 postinfection. In brief, induction of organ homogenate cytokine production was low or not increased in response to infection (tumor necrosis factor alpha [TNF-α] and IFN-γ), except for interleukin 1β (IL-1β), which largely reflected organ bacterial loads (see Fig. S1 in the supplemental material). The overall

low induction levels were not surprising; cytokines could be secreted by subsets of immune cells and act in an autocrine/paracrine manner, e.g., in tissue granulomas. As mentioned, we have previously characterized the C57BL/6 infection of strain MAH 104 in great detail (12). Similar to what we observed with MAH 104, MAH 11 infection induced organ pathology seen as disruption of splenic pulp structures, infiltration of immune cells, inflammatory foci (granulomas), and giant cell formation (Fig. S2). In summary, though, MAH 11 appears to be suitable to study mycobacterial disease mechanisms, as well as host responses, in a mouse infection model.

MAH virulence gene set. To identify genes required for MAH virulence, we infected six mice with our MAH library and analyzed bacterial loads from the spleen and liver (organs from two animals each were pooled, resulting in three spleen libraries and three liver libraries) after 26 days of infection. We sequenced the harvested libraries, which yielded saturation of 61.9% and 71.0% (combined over replicates) for spleen and liver, respectively (Table S1). We then defined the genetic requirement for infection using a TRANSIT-incorporated resampling algorithm for comparative analysis (52), comparing output data from sequenced libraries before and after infection. We identified 144 and 128 genes as required for spleen and liver infection, respectively (Data Set S1B). A total of 112 genes were required for survival in both organs (~80% overlap). Direct comparison of the spleen and liver data sets by resampling did not reveal any statistically significant differences, and hence, no genes uniquely required for colonization of either organ were identified. Among the core genes identified (found in both spleen and liver) were 51 previously identified in *Mtb* mouse model TnSeq experiments (16), including well-established mycobacterial virulence genes like *uvrABC* (the UvrABC endonuclease complex [55]), *secA2* (alternative ATPase of Sec secretion pathway [56]), *icl* (isocitrate lyase [57]), *bioA* (within the biotin biosynthesis pathway [58]), and *glcb* (malate synthase [59]). However, importantly, we identified 61 core genes (92 genes with spleen and liver genes combined) that were not previously detected by *Mtb* TnSeq virulence gene screening (Fig. 2D) (16). Some of these genes were found in genetic clusters, like six genes within the region encoding the type VII ESX-5 secretion system. Other genes were found in operons (for instance, *prcA*/*prcB*, *mav_3300*/*ripA*, and *mav_3691*/*rbfA*) or in close genomic vicinity (*mav_4154*/*4158*/*4159*/*4160*/*4163*). Strikingly, only three (<3%) core MAH virulence genes did not have a mutual ortholog in *Mtb* (Fig. 2D). Two of these genes, *mav_4273* and *mav_4274*, are potentially coexpressed, and both encode proline-proline-glutamic acid (PPE) family proteins. PPE proteins might show ambiguity in ortholog matching due to large duplications within the family. However, by BLAST search, the two PPE proteins have clear orthologs in MAC species (60), but not in other well-known mycobacterial species like *Mtb*, *M. bovis*, *M. abscessus*, or *M. leprae* (albeit both PPE proteins show a weak similarity to *M. marinum* PPE14 [*mmar_1235*] with 53 and 57% amino acid identity, respectively). The last of the three MAH virulence genes without *Mtb* mutual orthologs, *mav_4409*, encodes a putative acyltransferase.

As could be expected, most genes found on the two MAH 11 plasmids were nonessential for infection (Data Sets S1J to M); the only exceptions were an AAA-family ATPase on pMD1 (out of 162 ORFs), and two ORFs of unknown function on pMD2 (66 ORFs).

Identification of mutants in an organized MAH library. Vandewalle et al. developed a method where sequence tagging transposon library pools was used to bulk identify, by TnSeq, both the gene disrupted and the location of the mutation within an organized (plated) *M. bovis* BCG transposon library (61). Using a similar approach, we were able to map the specific locations of 2,696 unique transposon insertion mutations within 1,697 (34.8%) of the 4,881 MAH 11 ORFs (plasmid ORFs included) (Data Set S1N). Transposon insertion sites that mapped ambiguously to more than one plate, column, and/or row were disregarded; these might be due to a relatively high number of mutant duplicates in the picked library. A total of 3,161 wells had a unique clone, and only 155 wells had more than one mutant assigned to them (Data Set S1O). The latter

might be due to mutants clumping in colonies picked, incomplete sterilization of the robotic picking device between rounds of colony picking, or transposon insertions in repetitive or duplicated regions. To experimentally verify the correct locations of mutations, we sequenced 11 mutants picked from 11 wells (Table S2). All mutants had the transposon inserted at the location predicted by our TnSeq approach. Taken together, we identified the transposon insertion site and mapped the unambiguous location of 3,489 clones (including those in intergenic regions), providing access to a plethora of mutants to study the roles of the respective MAH genes.

***uvrB* is required for MAH virulence.** UvrABC is an enzyme complex involved in *Escherichia coli* nucleotide excision repair (62). The genes encoding the mycobacterial homologues of the three members of the complex, *uvrA*, *uvrB*, and *uvrC*, were all defined as virulence genes in our screen. *uvrB* has previously been implicated in *Mtb* virulence, via protection against host-mediated reactive nitrogen and oxygen intermediates (55). To verify the involvement of *uvrB* in MAH virulence, we infected mice with an available *uvrB* transposon mutant (*uvrB*::Tn) and complemented mutant for 26 days. The *uvrB*::Tn mutant showed reduced bacterial burden in infected mice compared to mice infected with wild-type (wt) MAH 11 strain and the complemented mutant (Fig. 5A and B). Neither the *uvrB* mutant nor the complemented mutant showed reduced fitness *in vitro* (Fig. 5E); hence, our results suggest that UvrB is required for full virulence in MAH in a mouse model.

A probable MFS transporter is required for MAH virulence. Next, we aimed to validate MAH determinants not previously implicated in mycobacterial virulence. A mutant of a probable major facilitator superfamily (MFS) transporter, MAV_1005 (ortholog of Rv0876c), showed attenuated growth in our virulence screen. When we subjected an MAH 11 transposon mutant of this transporter (*1005*::Tn) to mouse model infection, we saw a strong attenuation after 26 days of infection compared to the wt and the complemented mutant (Fig. 5A and B). Furthermore, the mutant, but not the complemented mutant, elicited a reduced MAH-specific $CD4^+$ effector T cell response from the host (Fig. 5C and D). The mutant did not show reduced fitness *in vitro* (Fig. 5E). Taken together, our results suggest that *mav_1005* is crucial for MAH virulence in a mouse model.

A hypothetical gene required for MAH virulence. Five genes located in close genomic vicinity (region spanning from *mav_4154* to *mav_4163* [Fig. 5F]) appeared as hits in our virulence screen. An insertion mutant of one of the genes, hypothetical gene *mav_4160* (*4160*::Tn), was subjected to a mouse model infection. After 26 days of infection, *4160*::Tn showed attenuated growth in both the liver and spleen (Fig. 5A and B), though the MAH-specific effector $CD4^+$ T cell response was not significantly reduced (Fig. 5C and D). The mutant did not show reduced fitness *in vitro* (Fig. 5E). Hence, our findings suggest that *mav_4160* is required for full MAH virulence in a mouse model. No obvious differences in cytokine production or tissue pathology were seen between the mutants tested (*uvrB*::Tn, *1005*::Tn, and *4160*::Tn) and the wt or between the mutants and complemented mutants (Fig. S1 and S2). Nevertheless, the overall organ pathology and IL-1β production grossly reflected bacterial loads, suggesting that these virulence genes might be required for intracellular growth (i.e., adapt to nutrient conditions of the host cells or combat host responses on an intracellular level), rather that affecting organ pathology directly.

DISCUSSION

Studying the role of genes by loss of function is a powerful approach to understanding how pathogens proliferate and avoid host elimination. We identified a virulent clinical isolate of MAH susceptible to genome-wide high-density gene disruption by ϕMycoMarT7-mediated transposon mutagenesis. The transposon library generated enabled us to define the MAH *in vitro* essential and virulence gene sets using a top-down discovery-based deep-sequencing approach. A total of 674 genes (essential and causing growth defect when disrupted) were identified as required for normal growth *in vitro* (15% of total genes, similar to the proportion of required genes in *Mtb*

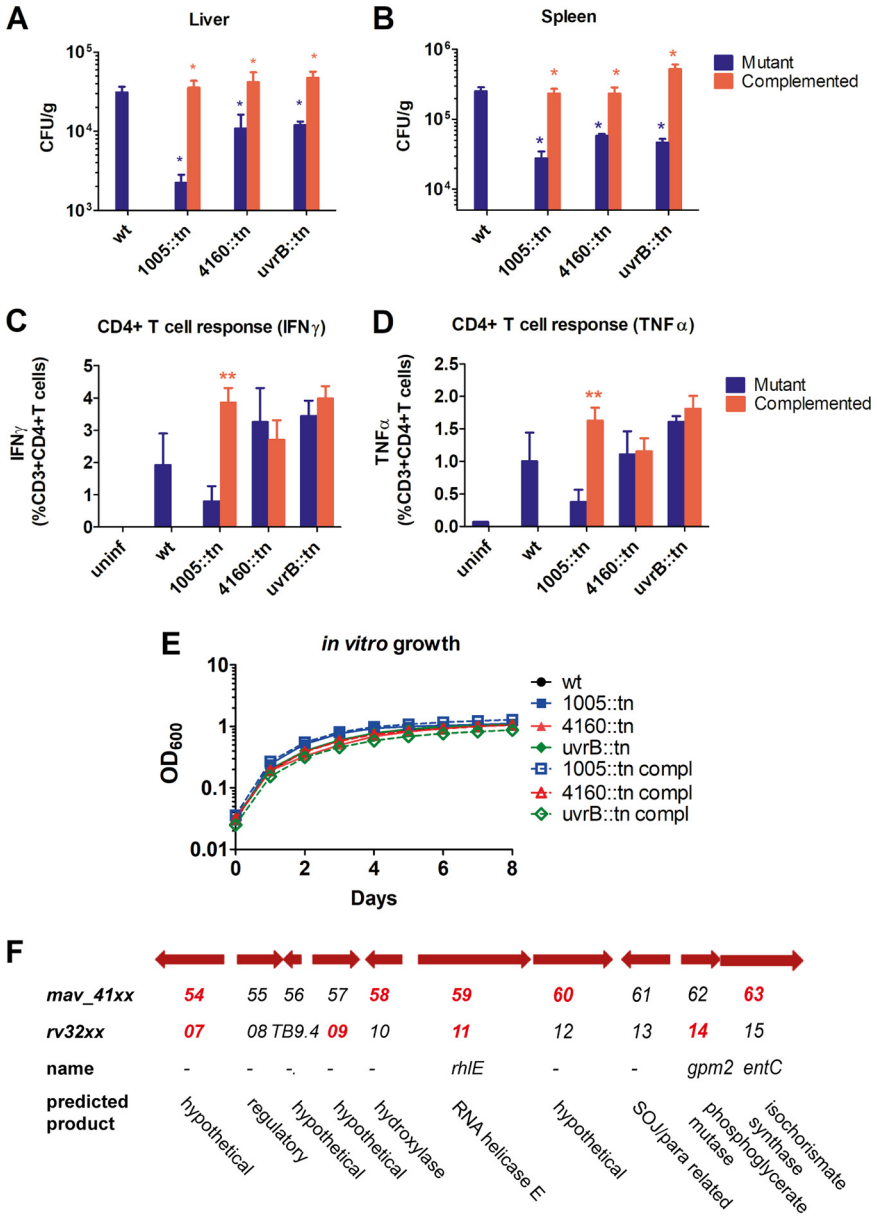

FIG 5 Validation of virulence genes. Mice were infected with wild-type (wt) MAH 11 or MAH 11 transposon insertion mutants with and without complementation. (A and B) After 26 days of infection, the bacterial burden in spleen (A) and liver (B) was determined by CFU per gram organ. Data show means plus SEM of three or four infected mice in each group. Values that are significantly different ($P \leq 0.05$) by one-tailed Mann Whitney U test are indicated by an asterisk (mutant compared to wt [blue asterisk] or mutant compared to complemented mutant [red asterisk]). (C and D) MAH-specific $CD4^+$ effector T cell response in mice infected with wt MAH 11 or MAH 11 transposon insertion mutants. At 26 days postinfection, splenocytes from all mice in each group were stimulated with MAH overnight, and frequencies of IFN-γ-producing (C) and TNF-α-producing (D) $CD4^+$ T helper cells were determined by flow cytometry. Data show means plus SEM. Values that are significantly different ($P \leq 0.01$) from the wt value by two-tailed unpaired Student's *t* test are indicated by two asterisks. (E) *In vitro* growth (7H9 medium) of wt MAH 11 and transposon insertion mutants with and without complementation. Data show means ± SEM for three replicate samples per condition. The results are representative of three independent experiments. (F) Genetic region spanning from *mav_4154-4163*. Hits from our virulence screen (*mav_41xx*) and previously published *Mtb* virulence screen (Rv32xx) (16) are shown in bold red type.

[53]). There was a substantial overlap (71%) of *in vitro* essential genes between MAH and *Mtb*, as well as many common virulence genes (e.g., *uvrABC*, *secA2*, *icl*) required for survival in a mouse model of infection. The majority of the virulence genes we identified were, however, novel relative to *Mtb* TnSeq virulence screening (16). Likewise,

several known *Mtb* virulence factors were not detected in our MAH screen (such as genes involved in cholesterol transport and catabolism, like mammalian cell entry operon [*mce*] 4, *hsaBCD*, and *fadE28-29* [63]), albeit it is important to note that the *Mtb* TnSeq virulence screen identified genes required after 10 and 45 days of infection (as opposed to the 26 days of infection for our MAH screen), potentially causing differences in observed virulence requirement. Surprisingly, though, even with 1,052 genes with no clear *Mtb* ortholog, only 3 of the MAH virulence genes were specific to MAH (i.e., did not have a mutual ortholog in the H37Rv genome). Two of these were PPE family proteins (*mav_4273/4*, found in MAC species but not *Mtb* [60]), which are unique to mycobacteria and associated with virulence, and some have been shown to be secreted by the ESX-5 secretion system in *M. marinum* and *Mtb* (64, 65). In fact, we observed six genes within the MAH *esx-5* gene cluster among our virulence genes (*mav_2916-2933*), strongly indicating a crucial role of ESX-5 during MAH infection. Interestingly, in *Mtb* and *M. marinum*, ESX-5 components are required for *in vitro* viability (19, 53), likely as a consequence of their essential role in outer membrane permeability, mediating uptake of nutrients and/or metabolites (66). The same ESX-5 components are dispensable in MAH *in vitro* but required during infection, suggesting that outer membrane permeability might be differently organized in this species. Even so, when we subjected an ESX-5 mutant (*eccA5*::Tn) to mouse infection, we did not see attenuated growth compared to the wt (see Fig. S3A, B and E in the supplemental material), perhaps due to insufficient disruption of gene function in this mutant (transposon insertion in the C terminus) or perhaps this particular gene is not required for ESX-5-mediated virulence in mice, as previously seen for *Mtb* (65). Intriguingly, though, we saw an increased $CD4^+$ T cell host response when *eccA5* was overexpressed (Fig. S3C and D). Taken together, it is possible that the two MAC-specific PPE proteins are secreted via the ESX-5 secretion system of MAH. These PPE proteins could be excellent candidates for targeted drug, vaccine, and/or diagnostic discovery for improved control of MAC infections.

MAH and *Mtb* are both able to persist in human macrophages; however, *Mav* is environmental and opportunistic, while *Mtb* is an obligate human pathogen. The relatively modest overlap between MAH and *Mtb* in mutually orthologous virulence genes (46%) compared to the overlap of *in vitro* essential genes (71%) might reflect different mechanisms of virulence. However, interestingly, many of the novel genes identified in our MAH virulence screen (i.e., not identified in the *Mtb* virulence screening [16]) have been experimentally proven to be required for *Mtb* virulence (exemplified by *prcA* and *prcB* genes encoding proteasome subunits and genes encoding components of the *esx-5* secretion system [65, 67]). This suggests that a portion of the genes we found unique to MAH virulence and that have *Mtb* mutual orthologs might be required for *Mtb* virulence as well. Even so, it is evident that when MAH and *Mtb* are subjected to the same selective conditions (*in vitro* growth on 7H10 agar or *in vivo* growth in C57BL/6 mice), MAH depends on very few genes that do not have mutual orthologs in *Mtb* (~4% and ~3%, respectively). Whether this is also true for other MAH isolates remains to be investigated. None of the genes within the major MAH 11 insertions (relative to MAH 104, listed in Table 1) were required for infection, and only four were essential *in vitro*. It has been shown that *M. marinum* customizes its virulence mechanisms to infect different animal cells (19). It is thus possible that, if subjected to infection of other animal models, a greater proportion of genes specific to MAH would be required.

Interestingly, we identified genes on the two plasmids, pMD1 and pMD2, defined as required for growth *in vitro* or *in vivo*. The *in vitro* growth defect seen in disruption of plasmid replication (*rep*) and partition (*parB*) genes might indicate that the presence of the two plasmids is required for efficient MAH proliferation, that disturbing plasmid replication/partition reduces the global fitness of the MAH cells, or perhaps most likely, that the disruptions cause an underrepresentation of the plasmids due to inefficient replication/partition (but with continued normal growth of the affected bacterial cells). It is currently unclear which role the three plasmid genes we found required *in vivo* might play during infection.

Using defined transposon mutants from our organized (plated) library, we validated a subset of our MAH virulence hits. We verified that the excision repair protein UvrB, a probable MFS transporter, and a hypothetical gene located within a genomic region of several identified virulence genes, are required for full MAH virulence. UvrB has previously been implicated in mycobacterial virulence (55), while the MFS transporter (*mav_1005*) and the hypothetical gene (*mav_4160*) were first validated as mycobacterial virulence factors by us. Of the six other virulence genes identified (based on MAH and *Mtb* screening) in the immediate vicinity of *mav_4160*, two encode hypothetical proteins, one encodes a hydroxylase, one encodes RNA helicase E (RhlE), one encodes isochorismate synthase (EntC), and one encodes phosphoglycerate mutase (Gmp2) (Fig. 5E). EntC was shown to be required for siderophore production in *M. smegmatis* (68), and might thus play a role in iron acquisition during infection. However, the mechanism of the MFS transporter, as well as *mav_4160* and the surrounding genes, in mycobacterial virulence remains to be elucidated.

Mav isolates exhibit high genetic variation (14, 43, 69, 70). In accordance, we registered several large-scale insertions and deletions when we compared the genomic sequence of MAH 11 to the genomic sequence of MAH 104. The movement of genetic material between organisms is mediated by, among other mechanisms, phage transduction, natural transformation, and plasmid conjugation (71). The cause (and effect) of *Mav* genomic plasticity is largely unknown. However, recently, mycobacterial conjugative plasmids have also been identified in *Mav* (48, 49). Interestingly, one of MAH 11's plasmids, pMD2, is almost identical to previously described *Mav* plasmid pMA100 (48). pMA100 was shown to transfer via conjugation between the slow-growing mycobacteria *Mav* and *M. kansasii* in a patient with a mixed infection (48). pMD2 might thus partake in genetic exchange between MAH 11 and other mycobacteria.

In conclusion, we identified a highly transformable MAH strain susceptible to ϕMycoMarT7-mediated transposon mutagenesis. This strain enabled genome-wide identification of *in vitro* essential and virulence genes in this species. On the basis of our screens, we identified growth and virulence genes specific to MAH, as well as shared with *Mtb*. MAH-specific genes might be excellent targets for MAC disease control, while shared genes might target related mycobacterial diseases as well. We validated two novel MAH genes required for infection. Since MAH 11 is used as a screening strain in mycobacterial drug discovery programs (38, 39), a comprehensive understanding of the genetic requirement for growth and infection of this strain is a direct asset for current initiatives aimed at discovering new antimycobacterial therapies.

MATERIALS AND METHODS

Strains and growth conditions. *Mycobacterium avium* subsp. *hominissuis* (MAH) strains used in this study were MAH 104 and MAH 11 (NCBI GenBank accession numbers CP000479 and CP035744, respectively). MAH strains were cultured in Middlebrook 7H9 (BD Difco) supplemented with 0.2% glycerol, 0.05% Tween 80, and 10% albumin-dextrose-catalase (ADC) (50 g bovine serum albumin [BSA] fraction V, 20 g dextrose, 8.5 g NaCl, 0.03 g catalase, distilled water [dH_2O] up to 1 liter) for liquid growth and in Middlebrook 7H10 (BD Difco) supplemented with 0.5% glycerol and 10% ADC for solid growth. For selection of transposon mutants, 20 μg/ml kanamycin and 0.1% Tween 80 was added to the 7H10 agar plate, the latter to simplify library harvest.

Genome sequencing and annotation. DNA from late-log-phase cultures of MAH 11 was extracted using a Masterpure DNA Purification kit (Epicentre), prepared using the TruSeq genome DNA sample preparation kit (Illumina, Inc.), and sequenced on an Illumina HiSeq 2500 instrument in paired-end mode with a read length of 125 bp. The genome sequence was assembled using a comparative assembly method, using MAH 104 as a reference sequence (see Text S1 for a detailed description of the assembly and annotation).

Transformation. Competent MAH cells were prepared as previously optimized for *M. avium* (*Mav*) (35). One hundred microliters of competent cells was electroporated with 2 μg plasmid DNA (pMSP12::cfp, kind gift from Christine Cosma and Lalita Ramakrishnan [72]) in a 2-mm cuvette at the following settings: 2.5 kV, 1,000 Ω, and 25 μF. Cells were recovered overnight and plated at serial dilutions for CFU counts. CFU counts of pMSP12::cfp-transformed bacteria selected on 7H10 with 20 μg/ml kanamycin were normalized to the CFU counts of transformed bacteria titered on 7H10 without antibiotics.

Growth curves. Wild-type (wt) MAH and mutants were grown in 7H9 medium until they reached stationary phase and then diluted to an optical density at 600 nm (OD_{600}) of 0.02 in triplicates of 200 μl 7H9 medium in microplate honeycomb wells (Oy Growth Curves Ab Ltd.). Growth was monitored over the course of 10 days in a Bioscreen growth curve reader (Oy Growth Curves Ab Ltd.) shaking at 37°C.

Generation of MAH transposon mutant library. The MAH high-density transposon mutant library was prepared using ϕMycoMarT7 as previously described for *M. tuberculosis* (*Mtb*) (73), with the exception of growing the bacterial culture to stationary phase as opposed to exponential phase prior to transduction. The amount of ϕMycoMarT7 added for transduction was increased coordinately with the increased bacterial density. Both the phage stock and bacterial culture were heated to 37°C before transduction. The library was incubated at 37°C on 7H10 plates with Tween 80 (0.1%) and kanamycin (20 μg/ml) for 2 to 3 weeks.

Transposon insertion sequencing. The transposon library was harvested and pooled by scraping 7H10 plates with 170,000 colonies. Total DNA was purified using Masterpure DNA purification kit (Epicentre) and prepared for transposon insertion sequencing (TnSeq) by PCR amplification of transposon-genome junctions and adapter ligation following the protocol in reference 51. The samples were sequenced on an Illumina GAII instrument, collecting around 10 million 54-bp paired-end reads per sample. The reads were processed using TPP in TRANSIT (52), which counts reads mapping to each TA dinucleotide site (after eliminating reads sharing the same template barcode [51]).

MAH *in vitro* essential gene set. Essential genes were identified using a hidden Markov model (HMM) (74), incorporated into TRANSIT (52). The HMM is a Bayesian statistical model that parses the genome into contiguous regions labeled as one of four states—essential (ES), nonessential (NE), growth defect (GD, suppressed insertion counts), or growth advantaged (GA) (insertion counts higher than average)—based on local insertion density and mean read count at TA sites. Thus, the label of each TA site is not determined as the maximum likelihood state independently at each site, but rather, it is the most probable sequence of states for the whole sequence taken together (computed using the Viterbi algorithm), and the call for the gene is based on the majority (or most frequent) call over the TA sites in the gene.

Mouse infection. For MAH 104 and MAH 11 infection experiments, groups of four C57BL/6 mice were infected intraperitoneally with 5×10^7 CFU/mouse as previously described (12). On day 22 and day 50 postinfection, MAH-specific effector T cell responses and bacterial load were analyzed. The numbers of CFU per gram of organ were determined by plating serial dilutions of spleen and liver homogenates on 7H10 plates. For the virulence gene screen, six mice were infected intraperitoneally with 6×10^7 CFU/mouse of the MAH 11 transposon mutant library. After 22 days of infection, mice were sacrificed, and the livers and spleens were harvested, homogenized, and plated on 7H10 (livers and spleens from two mice were pooled to make one library, resulting in three liver and three spleen libraries in total from the six mice). After 2 to 3 weeks at 37°C, the colonies were scraped and DNA was prepared for sequencing as described above for TnSeq. For *in vivo* validation experiments of virulence genes, groups of four or five C57BL/6 mice were infected intraperitoneally with (approximately) 7.5×10^7 CFU/mouse MAH 11 wt or MAH 11 transposon insertion mutants. On day 26 postinfection, bacterial load in liver and spleen, MAH-specific effector T cell responses, cytokine levels in organs and serum, and histopathology were analyzed. Statistically significant differences between mutants and the wt were determined using the two-tailed unpaired Student's *t* test (T cell responses) or one-tailed Mann-Whitney U test (bacterial load by CFU) using Prism GraphPad version 5.

MAH-specific T cell response. Isolated splenocytes from infected mice were stimulated overnight with MAH (multiplicity of infection [MOI] of 3:1); protein transport inhibitor cocktail (eBioscience) was added for the last 4 h of incubation. Unstimulated cells were used as controls. Cells were harvested and stained with Fixable Viability Dye eFluor 780 (eBioscience) and fluorescence-labeled monoclonal antibodies against CD3 (fluorescein isothiocyanate [FITC]; eBioscience) and CD4 (Alexa Fluor 700 or Brilliant Violet 605; both from BioLegend). After fixation and permeabilization, intracellular cytokine staining was performed with fluorescent monoclonal antibody against gamma interferon (IFN-γ) (phycoerythrin; eBioscience) and tumor necrosis factor alpha (TNF-α) (allophycocyanin; BioLegend). Cells were analyzed by flow cytometry on a BD LSR II flow cytometer (BD Biosciences), and data were subsequently analyzed with FlowJo (FlowJo, LLC) and GraphPad Prism (GraphPad Software, Inc.) software. Frequencies of IFN-γ- and TNF-α-producing $CD4^+$ effector T cells were analyzed from forward scatter (FSC)/side scatter (SSC)-gated, viable $CD3^+$ $CD4^+$ T cells. The method is described in further detail in reference 12.

Cytokine measurements. Interleukin 1β (IL-1β), IFN-γ, and TNF-α levels were analyzed in serum as well as spleen and liver homogenates from infected mice using a custom-made ProcartaPlex immunoassay panel (Affymetrix, eBioscience) according to the manufacturer's protocol.

Histopathology. Standard hematoxylin and eosin staining of spleen and liver sections was performed at the Cellular and Molecular Imaging Core Facility (CMIC) at Norwegian University of Science and Technology (NTNU) as described previously (12). Images were acquired with a Nikon E400 microscope and NIS-Elements BR imaging software (Nikon Instruments, Melville, NY, USA).

MAH virulence gene set. For comparative analysis between the *in vitro*-selected and the *in vivo* (mouse infection)-selected transposon libraries, the TRANSIT-incorporated "resampling" algorithm was used (52). Resampling is analogous to a permutation test, examining whether the sum of transposon insertion read counts differs significantly between conditions.

Bulk identification of transposon insertion sites in the organized MAH library. A total of 9,216 colonies were picked (384-well format), tagged, and pooled before sequencing on an Illumina HiSeq 2500. The sequences were then subjected to simultaneous detection of location and gene disruption (see detailed description in Text S1 and Table S3 in the supplemental material).

Verification of mutants by Sanger sequencing. Total DNA was isolated using Masterpure Complete DNA Isolation kit (Epicentre). Sanger sequencing was performed using genomic DNA (gDNA) as the template prepared with BigDye Terminator Cycle Sequencing kit v.1.1 (Thermo Fisher); sequencing was conducted with 60 cycles of PCR, with 1 cycle consisting of 30 s at 95°C, 30 s at 52°C, and 4 min at 60°C,

and primer KanSeq2 (CTTCCTCGTGCTTTACGG) reading directly into the gDNA. Samples were purified using BigDye XTerminator kit (Applied Biosystems) and sequenced on an ABI130xl.

Complementation of transposon insertion mutants. Plasmids for complementation of transposon insertion mutations were constructed by cloning the wt version of the disrupted gene into the mycobacterium-*Escherichia coli* shuttle vector pMV261 (75) (swapping the kanamycin resistance gene of pMV261 with the hygromycin resistance gene of pUV15TetORm [76]) for constitutive expression (for more details, see Text S1).

Ethics statement. The protocols on animal work were approved by the Norwegian Animal Research Authorities (Forsøksdyrutvalget, FOTS ID 5955). All procedures involving mouse experiments were conducted in accordance with institutional guidelines, national legislation, and the Directive of the European Convention for the protection of vertebrate animals used for scientific purposes (2010/63/EU).

SUPPLEMENTAL MATERIAL

Supplemental material for this article may be found at https://doi.org/10.1128/mSystems.00402-19.

TEXT S1, PDF file, 0.4 MB.
FIG S1, TIF file, 0.5 MB.
FIG S2, JPG file, 2.6 MB.
FIG S3, TIF file, 0.6 MB.
TABLE S1, PDF file, 0.1 MB.
TABLE S2, PDF file, 0.1 MB.
TABLE S3, PDF file, 0.1 MB.
DATA SET S1, XLSX file, 1.6 MB.

ACKNOWLEDGMENTS

This work was partly supported by the Research Council of Norway (www.forskningsradet.no) through its Centers of Excellence funding scheme, project number 223255/F50 (THF/CEMIR), and through project number 249901 (M.S.D.), and the Liaison Committee between Norwegian University of Science and Technology (NTNU) and the Central Norway Regional Health Authority (helse-midt.no) (T.H.F., M.H., and M.S.).

The funders had no role in study design, data collection and analysis, decision to publish, or preparation of the manuscript.

We thank Jun-Rong Wei, Jung-Yien Chien, and Po-Ren Hsueh for providing clinical MAH isolates from the National Taiwan University Hospital, the Medical Genetics Department at St. Olavs Hospital for assistance with Sanger sequencing, the Cellular and Molecular Imaging Core Facility (CMIC) at NTNU for histopathology staining and personnel at the Comparative Medicine Core Facility (CoMed) at NTNU for assistance in animal experiments. CMIC and CoMed are funded by the Faculty of Medicine and Health Science at NTNU and Central Norway Regional Health Authority. We acknowledge the help of the Texas A&M Sequencing Center (Genomics & Bioinformatics Service; Charlie Johnson, director).

REFERENCES

1. Prevots DR, Marras TK. 2015. Epidemiology of human pulmonary infection with nontuberculous mycobacteria: a review. Clin Chest Med 36:13–34. https://doi.org/10.1016/j.ccm.2014.10.002.
2. Turenne CY, Wallace R, Jr, Behr MA. 2007. Mycobacterium avium in the postgenomic era. Clin Microbiol Rev 20:205–229. https://doi.org/10.1128/CMR.00036-06.
3. Rindi L, Garzelli C. 2014. Genetic diversity and phylogeny of Mycobacterium avium. Infect Genet Evol 21:375–383. https://doi.org/10.1016/j.meegid.2013.12.007.
4. Falkinham JO, III.. 1996. Epidemiology of infection by nontuberculous mycobacteria. Clin Microbiol Rev 9:177–215. https://doi.org/10.1128/CMR.9.2.177.
5. Thomson RM, Yew WW. 2009. When and how to treat pulmonary non-tuberculous mycobacterial diseases. Respirology 14:12–26. https://doi.org/10.1111/j.1440-1843.2008.01408.x.
6. Appelberg R. 2006. Pathogenesis of Mycobacterium avium infection: typical responses to an atypical mycobacterium? Immunol Res 35:179–190. https://doi.org/10.1385/IR:35:3:179.
7. Awuh JA, Flo TH. 2017. Molecular basis of mycobacterial survival in macrophages. Cell Mol Life Sci 74:1625–1648. https://doi.org/10.1007/s00018-016-2422-8.
8. Awuh JA, Haug M, Mildenberger J, Marstad A, Do CP, Louet C, Stenvik J, Steigedal M, Damas JK, Halaas O, Flo TH. 2015. Keap1 regulates inflammatory signaling in Mycobacterium avium-infected human macrophages. Proc Natl Acad Sci U S A 112:E4272–E4280. https://doi.org/10.1073/pnas.1423449112.
9. Ernst JD. 2012. The immunological life cycle of tuberculosis. Nat Rev Immunol 12:581–591. https://doi.org/10.1038/nri3259.
10. Gidon A, Asberg SE, Louet C, Ryan L, Haug M, Flo TH. 2017. Persistent mycobacteria evade an antibacterial program mediated by phagolysosomal TLR7/8/MyD88 in human primary macrophages. PLoS Pathog 13:e1006551. https://doi.org/10.1371/journal.ppat.1006551.
11. Halaas O, Steigedal M, Haug M, Awuh JA, Ryan L, Brech A, Sato S, Husebye H, Cangelosi GA, Akira S, Strong RK, Espevik T, Flo TH. 2010. Intracellular Mycobacterium avium intersect transferrin in the Rab11$^+$ recycling endocytic pathway and avoid lipocalin 2 trafficking to the lysosomal pathway. J Infect Dis 201:783–792. https://doi.org/10.1086/650493.

12. Haug M, Awuh JA, Steigedal M, Frengen Kojen J, Marstad A, Nordrum IS, Halaas O, Flo TH. 2013. Dynamics of immune effector mechanisms during infection with Mycobacterium avium in C57BL/6 mice. Immunology 140:232–243. https://doi.org/10.1111/imm.12131.
13. Champion PA, Champion MM, Manzanillo P, Cox JS. 2009. ESX-1 secreted virulence factors are recognized by multiple cytosolic AAA ATPases in pathogenic mycobacteria. Mol Microbiol 73:950–962. https://doi.org/10.1111/j.1365-2958.2009.06821.x.
14. Uchiya K, Tomida S, Nakagawa T, Asahi S, Nikai T, Ogawa K. 2017. Comparative genome analyses of Mycobacterium avium reveal genomic features of its subspecies and strains that cause progression of pulmonary disease. Sci Rep 7:39750. https://doi.org/10.1038/srep39750.
15. van Opijnen T, Bodi KL, Camilli A. 2009. Tn-seq: high-throughput parallel sequencing for fitness and genetic interaction studies in microorganisms. Nat Methods 6:767–772. https://doi.org/10.1038/nmeth.1377.
16. Zhang YJJ, Reddy MC, Ioerger TR, Rothchild AC, Dartois V, Schuster BM, Trauner A, Wallis D, Galaviz S, Huttenhower C, Sacchettini JC, Behar SM, Rubin EJ. 2013. Tryptophan biosynthesis protects mycobacteria from CD4 T-cell-mediated killing. Cell 155:1296–1308. https://doi.org/10.1016/j.cell.2013.10.045.
17. Zhang YJJ, Ioerger TR, Huttenhower C, Long JE, Sassetti CM, Sacchettini JC, Rubin EJ. 2012. Global assessment of genomic regions required for growth in Mycobacterium tuberculosis. PLoS Pathog 8:e1002946. https://doi.org/10.1371/journal.ppat.1002946.
18. Griffin JE, Gawronski JD, DeJesus MA, Ioerger TR, Akerley BJ, Sassetti CM. 2011. High-resolution phenotypic profiling defines genes essential for mycobacterial growth and cholesterol catabolism. PLoS Pathog 7:e1002251. https://doi.org/10.1371/journal.ppat.1002251.
19. Weerdenburg EM, Abdallah AM, Rangkuti F, El Ghany MA, Otto TD, Adroub SA, Molenaar D, Ummels R, ter Veen K, van Stempvoort G, van der Sar AM, Ali S, Langridge GC, Thomson NR, Pain A, Bitter W. 2015. Genome-wide transposon mutagenesis indicates that Mycobacterium marinum customizes its virulence mechanisms for survival and replication in different hosts. Infect Immun 83:1778–1788. https://doi.org/10.1128/IAI.03050-14.
20. Wang J, Pritchard JR, Kreitmann L, Montpetit A, Behr MA. 2014. Disruption of Mycobacterium avium subsp paratuberculosis-specific genes impairs in vivo fitness. BMC Genomics 15:415. https://doi.org/10.1186/1471-2164-15-415.
21. Motamedi N, Danelishvili L, Bermudez LE. 2014. Identification of Mycobacterium avium genes associated with resistance to host antimicrobial peptides. J Med Microbiol 63:923–930. https://doi.org/10.1099/jmm.0.072744-0.
22. Li YJ, Danelishvili L, Wagner D, Petrofsky M, Bermudez LE. 2010. Identification of virulence determinants of Mycobacterium avium that impact on the ability to resist host killing mechanisms. J Med Microbiol 59:8–16. https://doi.org/10.1099/jmm.0.012864-0.
23. Li Y, Miltner E, Wu M, Petrofsky M, Bermudez LE. 2005. A Mycobacterium avium PPE gene is associated with the ability of the bacterium to grow in macrophages and virulence in mice. Cell Microbiol 7:539–548. https://doi.org/10.1111/j.1462-5822.2004.00484.x.
24. Danelishvili L, Wu M, Stang B, Harriff M, Cirillo SLG, Cirillo S, Cirillo JD, Cirillo J, Bildfell R, Arbogast B, Bermudez LE. 2007. Identification of Mycobacterium avium pathogenicity island important for macrophage and amoeba infection. Proc Natl Acad Sci U S A 104:11038–11043. https://doi.org/10.1073/pnas.0610746104.
25. Bermudez LE, Danelishvili L, Babrack L, Pham T. 2015. Evidence for genes associated with the ability of Mycobacterium avium subsp. hominissuis to escape apoptotic macrophages. Front Cell Infect Microbiol 5:63. https://doi.org/10.3389/fcimb.2015.00063.
26. Bermudez LE, Rose SJ, Everman JL, Ziaie NR. 2018. Establishment of a host-to-host transmission model for Mycobacterium avium subsp. hominissuis using Caenorhabditis elegans and identification of colonization-associated genes. Front Cell Infect Microbiol 8:123. https://doi.org/10.3389/fcimb.2018.00123.
27. Rose SJ, Bermudez LE. 2016. Identification of bicarbonate as a trigger and genes involved with extracellular DNA export in mycobacterial biofilms. mBio 7:e01597-16. https://doi.org/10.1128/mBio.01597-16.
28. Khattak FA, Kumar A, Kamal E, Kunisch R, Lewin A. 2012. Illegitimate recombination: an efficient method for random mutagenesis in Mycobacterium avium subsp. hominissuis. BMC Microbiol 12:204. https://doi.org/10.1186/1471-2180-12-204.
29. Yamazaki Y, Danelishvili L, Wu M, Macnab M, Bermudez LE. 2006. Mycobacterium avium genes associated with the ability to form a biofilm. Appl Environ Microbiol 72:819–825. https://doi.org/10.1128/AEM.72.1.819-825.2006.
30. Horan KL, Freeman R, Weigel K, Semret M, Pfaller S, Covert TC, van Soolingen D, Leao SC, Behr MA, Cangelosi GA. 2006. Isolation of the genome sequence strain Mycobacterium avium 104 from multiple patients over a 17-year period. J Clin Microbiol 44:783–789. https://doi.org/10.1128/JCM.44.3.783-789.2006.
31. Uchiya K, Takahashi H, Yagi T, Moriyama M, Inagaki T, Ichikawa K, Nakagawa T, Nikai T, Ogawa K. 2013. Comparative genome analysis of Mycobacterium avium revealed genetic diversity in strains that cause pulmonary and disseminated disease. PLoS One 8:e71831. https://doi.org/10.1371/journal.pone.0071831.
32. Pope WH, Ferreira CM, Jacobs-Sera D, Benjamin RC, Davis AJ, DeJong RJ, Elgin SCR, Guilfoile FR, Forsyth MH, Harris AD, Harvey SE, Hughes LE, Hynes PM, Jackson AS, Jalal MD, MacMurray EA, Manley CM, McDonough MJ, Mosier JL, Osterbann LJ, Rabinowitz HS, Rhyan CN, Russell DA, Saha MS, Shaffer CD, Simon SE, Sims EF, Tovar IG, Weisser EG, Wertz JT, Weston-Hafer KA, Williamson KE, Zhang B, Cresawn SG, Jain P, Piuri M, Jacobs WR, Hendrix RW, Hatfull GF. 2011. Cluster K mycobacteriophages: insights into the evolutionary origins of mycobacteriophage TM4. PLoS One 6:e26750. https://doi.org/10.1371/journal.pone.0026750.
33. Rathnaiah G, Bannantine JP, Bayles DO, Zinniel DK, Stabel JR, Grohn YT, Barletta RG. 2016. Analysis of Mycobacterium avium subsp. paratuberculosis mutant libraries reveals loci-dependent transposition biases and strategies to novel mutant discovery. Microbiology 162:633. https://doi.org/10.1099/mic.0.000258.
34. Sassetti CM, Boyd DH, Rubin EJ. 2001. Comprehensive identification of conditionally essential genes in mycobacteria. Proc Natl Acad Sci U S A 98:12712–12717. https://doi.org/10.1073/pnas.231275498.
35. Lee SH, Cheung M, Irani V, Carroll JD, Inamine JM, Howe WR, Maslow JN. 2002. Optimization of electroporation conditions for Mycobacterium avium. Tuberculosis (Edinb) 82:167–174. https://doi.org/10.1054/tube.2002.0335.
36. Madiraju M, Qin MH, Yamamoto K, Atkinson MAL, Rajagopalan M. 1999. The dnaA gene region of Mycobacterium avium and the autonomous replication activities of its 5′ and 3′ flanking regions. Microbiology 145:2913–2921. https://doi.org/10.1099/00221287-145-10-2913.
37. Foleythomas EM, Whipple DL, Bermudez LE, Barletta RG. 1995. Phage infection, transfection and transformation of Mycobacterium avium complex and Mycobacterium paratuberculosis. Microbiology 141:1173–1181. https://doi.org/10.1099/13500872-141-5-1173.
38. Moreira W, Lim JJ, Yeo SY, Ramanujulu PM, Dymock BW, Dick T. 2016. Fragment-based whole cell screen delivers hits against M. tuberculosis and non-tuberculous mycobacteria. Front Microbiol 7:1392. https://doi.org/10.3389/fmicb.2016.01392.
39. Yang TM, Moreira W, Nyantakyi SA, Chen H, Aziz DB, Go ML, Dick T. 2017. Amphiphilic indole derivatives as antimycobacterial agents: structure-activity relationships and membrane targeting properties. J Med Chem 60:2745–2763. https://doi.org/10.1021/acs.jmedchem.6b01530.
40. Bardarov S, Kriakov J, Carriere C, Yu S, Vaamonde C, McAdam RA, Bloom BR, Hatfull GF, Jacobs WR. 1997. Conditionally replicating mycobacteriophages: a system for transposon delivery to Mycobacterium tuberculosis. Proc Natl Acad Sci U S A 94:10961–10966. https://doi.org/10.1073/pnas.94.20.10961.
41. Krzywinska E, Bhatnagar S, Sweet L, Chatterjee D, Schorey JS. 2005. Mycobacterium avium 104 deleted of the methyltransferase D gene by allelic replacement lacks serotype-specific glycopeptidolipids and shows attenuated virulence in mice. Mol Microbiol 56:1262–1273. https://doi.org/10.1111/j.1365-2958.2005.04608.x.
42. Yee M, Klinzing D, Wei JR, Gengenbacher M, Rubin EJ, Chien JY, Hsueh PR, Dick T. 2017. Draft genome sequence of Mycobacterium avium 11. Genome Announc 5:e00766-17. https://doi.org/10.1128/genomeA.00766-17.
43. Semret M, Zhai G, Mostowy S, Cleto C, Alexander D, Cangelosi G, Cousins D, Collins DM, van Soolingen D, Behr MA. 2004. Extensive genomic polymorphism within Mycobacterium avium. J Bacteriol 186:6332–6334. https://doi.org/10.1128/JB.186.18.6332-6334.2004.
44. Wu CW, Glasner J, Collins M, Naser S, Talaat AM. 2006. Whole-genome plasticity among Mycobacterium avium subspecies: insights from comparative genomic hybridizations. J Bacteriol 188:711–723. https://doi.org/10.1128/JB.188.2.711-723.2006.
45. Guerrero C, Bernasconi C, Burki D, Bodmer T, Telenti A. 1995. A novel insertion element from Mycobacterium avium, Is1245, is a specific target for analysis of strain relatedness. J Clin Microbiol 33:304–307.

46. Kunze ZM, Wall S, Appelberg R, Silva MT, Portaels F, Mcfadden JJ. 1991. Is901, a new member of a widespread class of atypical insertion sequences, is associated with pathogenicity in Mycobacterium avium. Mol Microbiol 5:2265–2272. https://doi.org/10.1111/j.1365-2958.1991.tb02157.x.
47. Tatusova T, DiCuccio M, Badretdin A, Chetvernin V, Nawrocki EP, Zaslavsky L, Lomsadze A, Pruitt K, Borodovsky M, Ostell J. 2016. NCBI prokaryotic genome annotation pipeline. Nucleic Acids Res 44:6614–6624. https://doi.org/10.1093/nar/gkw569.
48. Rabello MCDS, Matsumoto CK, de Almeida LGP, Menendez MC, de Oliveira RS, Silva RM, Garcia MJ, Leão SC. 2012. First description of natural and experimental conjugation between mycobacteria mediated by a linear plasmid. PLoS One 7:e29884. https://doi.org/10.1371/journal.pone.0029884.
49. Ummels R, Abdallah AM, Kuiper V, Aajoud A, Sparrius M, Naeem R, Spaink HP, van Soolingen D, Pain A, Bitter W. 2014. Identification of a novel conjugative plasmid in mycobacteria that requires both type IV and type VII secretion. mBio 5:e01744-14. https://doi.org/10.1128/mBio.01744-14.
50. Rubin EJ, Akerley BJ, Novik VN, Lampe DJ, Husson RN, Mekalanos JJ. 1999. In vivo transposition of mariner-based elements in enteric bacteria and mycobacteria. Proc Natl Acad Sci U S A 96:1645–1650. https://doi.org/10.1073/pnas.96.4.1645.
51. Long JE, DeJesus M, Ward D, Baker RE, Ioerger T, Sassetti CM. 2015. Identifying essential genes in Mycobacterium tuberculosis by global phenotypic profiling. Methods Mol Biol 1279:79–95. https://doi.org/10.1007/978-1-4939-2398-4_6.
52. DeJesus MA, Ambadipudi C, Baker R, Sassetti C, Ioerger TR. 2015. TRANSIT–a software tool for Himar1 TnSeq analysis. PLoS Comput Biol 11:e1004401. https://doi.org/10.1371/journal.pcbi.1004401.
53. DeJesus MA, Gerrick ER, Xu W, Park SW, Long JE, Boutte CC, Rubin EJ, Schnappinger D, Ehrt S, Fortune SM, Sassetti CM, Ioerger TR. 2017. Comprehensive essentiality analysis of the Mycobacterium tuberculosis genome via saturating transposon mutagenesis. mBio 8:e02133-16. https://doi.org/10.1128/mBio.02133-16.
54. Saunders BM, Cheers C. 1995. Inflammatory response following intranasal infection with Mycobacterium avium complex: role of T-cell subsets and gamma interferon. Infect Immun 63:2282–2287.
55. Darwin KH, Nathan CF. 2005. Role for nucleotide excision repair in virulence of Mycobacterium tuberculosis. Infect Immun 73:4581–4587. https://doi.org/10.1128/IAI.73.8.4581-4587.2005.
56. Kurtz S, McKinnon KP, Runge MS, Ting JPY, Braunstein M. 2006. The SecA2 secretion factor of Mycobacterium tuberculosis promotes growth in macrophages and inhibits the host immune response. Infect Immun 74:6855–6864. https://doi.org/10.1128/IAI.01022-06.
57. McKinney JD, Honer zu Bentrup K, Munoz-Elias EJ, Miczak A, Chen B, Chan WT, Swenson D, Sacchettini JC, Jacobs WR, Jr, Russell DG. 2000. Persistence of Mycobacterium tuberculosis in macrophages and mice requires the glyoxylate shunt enzyme isocitrate lyase. Nature 406:735–738. https://doi.org/10.1038/35021074.
58. Kar R, Nangpal P, Mathur S, Singh S, Tyagi AK. 2017. bioA mutant of Mycobacterium tuberculosis shows severe growth defect and imparts protection against tuberculosis in guinea pigs. PLoS One 12:e0179513. https://doi.org/10.1371/journal.pone.0179513.
59. Puckett S, Trujillo C, Wang Z, Eoh H, Ioerger TR, Krieger I, Sacchettini J, Schnappinger D, Rhee KY, Ehrt S. 2017. Glyoxylate detoxification is an essential function of malate synthase required for carbon assimilation in Mycobacterium tuberculosis. Proc Natl Acad Sci U S A 114:E2225–E2232. https://doi.org/10.1073/pnas.1617655114.
60. Mackenzie N, Alexander DC, Turenne CY, Behr MA, De Buck JM. 2009. Genomic comparison of PE and PPE genes in the Mycobacterium avium complex. J Clin Microbiol 47:1002–1011. https://doi.org/10.1128/JCM.01313-08.
61. Vandewalle K, Festjens N, Plets E, Vuylsteke M, Saeys Y, Callewaert N. 2015. Characterization of genome-wide ordered sequence-tagged Mycobacterium mutant libraries by Cartesian pooling-coordinate sequencing. Nat Commun 6:7106. https://doi.org/10.1038/ncomms8106.
62. Truglio JJ, Croteau DL, Van Houten B, Kisker C. 2006. Prokaryotic nucleotide excision repair: the UvrABC system. Chem Rev 106:233–252. https://doi.org/10.1021/cr040471u.
63. Wilburn KM, Fieweger RA, VanderVen BC. 2018. Cholesterol and fatty acids grease the wheels of Mycobacterium tuberculosis pathogenesis. Pathog Dis 76:2. https://doi.org/10.1093/femspd/fty021.
64. Abdallah AM, Verboom T, Weerdenburg EM, Gey van Pittius NC, Mahasha PW, Jimenez C, Parra M, Cadieux N, Brennan MJ, Appelmelk BJ, Bitter W. 2009. PPE and PE_PGRS proteins of Mycobacterium marinum are transported via the type VII secretion system ESX-5. Mol Microbiol 73:329–340. https://doi.org/10.1111/j.1365-2958.2009.06783.x.
65. Bottai D, Di Luca M, Majlessi L, Frigui W, Simeone R, Sayes F, Bitter W, Brennan MJ, Leclerc C, Batoni G, Campa M, Brosch R, Esin S. 2012. Disruption of the ESX-5 system of Mycobacterium tuberculosis causes loss of PPE protein secretion, reduction of cell wall integrity and strong attenuation. Mol Microbiol 83:1195–1209. https://doi.org/10.1111/j.1365-2958.2012.08001.x.
66. Ates LS, Ummels R, Commandeur S, van de Weerd R, Sparrius M, Weerdenburg E, Alber M, Kalscheuer R, Piersma SR, Abdallah AM, Abd El Ghany M, Abdel-Haleem AM, Pain A, Jiménez CR, Bitter W, Houben ENG. 2015. Essential role of the ESX-5 secretion system in outer membrane permeability of pathogenic mycobacteria. PLoS Genet 11:e1005190. https://doi.org/10.1371/journal.pgen.1005190.
67. Blumenthal A, Trujillo C, Ehrt S, Schnappinger D. 2010. Simultaneous analysis of multiple Mycobacterium tuberculosis knockdown mutants in vitro and in vivo. PLoS One 5:e15667. https://doi.org/10.1371/journal.pone.0015667.
68. Nagachar N, Ratledge C. 2010. Roles of trpE2, entC and entD in salicylic acid biosynthesis in Mycobacterium smegmatis. FEMS Microbiol Lett 308:159–165. https://doi.org/10.1111/j.1574-6968.2010.02004.x.
69. Oliveira RS, Sircili MP, Oliveira EMD, Balian SC, Ferreira-Neto JS, Leão SC. 2003. Identification of Mycobacterium avium genotypes with distinctive traits by combination of IS1245-based restriction fragment length polymorphism and restriction analysis of hsp65. J Clin Microbiol 41:44–49. https://doi.org/10.1128/jcm.41.1.44-49.2003.
70. Kannan N, Lai YP, Haug M, Lilleness MK, Bakke SS, Marstad A, Hov H, Naustdal T, Afset JE, Ioerger TR, Flo TH, Steigedal M. 2019. Genetic variation/evolution and differential host responses resulting from in-patient adaptation of Mycobacterium avium. Infect Immun 87:e00323-18. https://doi.org/10.1128/IAI.00323-18.
71. Soucy SM, Huang JL, Gogarten JP. 2015. Horizontal gene transfer: building the web of life. Nat Rev Genet 16:472–482. https://doi.org/10.1038/nrg3962.
72. Cosma CL, Humbert O, Ramakrishnan L. 2004. Superinfecting mycobacteria home to established tuberculous granulomas. Nat Immunol 5:828–835. https://doi.org/10.1038/ni1091.
73. Majumdar G, Mbau R, Singh V, Warner DF, Dragset MS, Mukherjee R. 2017. Genome-wide transposon mutagenesis in Mycobacterium tuberculosis and Mycobacterium smegmatis. Methods Mol Biol 1498:321–335. https://doi.org/10.1007/978-1-4939-6472-7_21.
74. DeJesus MA, Ioerger TR. 2013. A Hidden Markov Model for identifying essential and growth-defect regions in bacterial genomes from transposon insertion sequencing data. BMC Bioinformatics 14:303. https://doi.org/10.1186/1471-2105-14-303.
75. Stover CK, de la Cruz VF, Fuerst TR, Burlein JE, Benson LA, Bennett LT, Bansal GP, Young JF, Lee MH, Hatfull GF, Snapper SB, Barletta RG, Jacobs WR, Bloom BR. 1991. New use of BCG for recombinant vaccines. Nature 351:456–460. https://doi.org/10.1038/351456a0.
76. Ehrt S, Guo XV, Hickey CM, Ryou M, Monteleone M, Riley LW, Schnappinger D. 2005. Controlling gene expression in mycobacteria with anhydrotetracycline and Tet repressor. Nucleic Acids Res 33:e21. https://doi.org/10.1093/nar/gni013.
77. Treangen TJ, Messeguer X. 2006. M-GCAT: interactively and efficiently constructing large-scale multiple genome comparison frameworks in closely related species. BMC Bioinformatics 7:433. https://doi.org/10.1186/1471-2105-7-433.